ANALYTICAL TECHNIQUES FOR MAGNETICALLY INDUCED VIBRATION IN BRUSHLESS PERMANENT MAGNET MOTORS

Ungtae Kim and D.K. Lieu
Pacific Rim Electro-Mechanical Laboratory
Department of Mechanical Engineering
University of California, Berkeley

ABSTRACT

This paper discusses an analytical method for predicting the force imbalance and cogging torque in a radial field permanent magnet motor. Explicit forms of the force imbalance and cogging torque expressions are derived based on a two dimensional model taking account of the effects of magnetic flux fringing at the stator slots. The Maxwell stress method is directly used for the force calculation. Dynamic characteristics of the force imbalance and cogging torque are explained in terms of the frequency content. Fast design criteria are suggested for motors used mostly in hard disk drives, from a vibration control viewpoint.

I. Introduction

The technology trends in rotating magnetic recording systems include high media data transfer rate and high track density, as well as small form factor for portable computer applications. These trends require spindle motors running at a very high speed with minimized force imbalance and cogging torque. The use of permanent magnetic materials with high maximum energy-products and the technology trends together have a great effect on motor design requirements, with respect to vibration reduction and very constant rotation speeds.

Force imbalance and cogging torque are two major problems related to electromagnetic design of spindle motors, from a vibration viewpoint. Force imbalance is defined as the global radial force acting on the stator or the rotor. This force is the result of unbalanced magnetic field distribution. There are several factors causing the imbalance of the field; for example, the eccentricity of the rotor and stator, the imbalance of the magnetic field in magnetically asymmetric motors, and unbalanced phase current excitation that depends on the phase winding patterns and connections, according to Chao, et al. [1996]. These factors may result from the quality of the motor components in assembling process and may also arise inherently from a design with a special purpose, as in 8-pole/9-slot motors, which are widely used for spindle motors in current hard disk drives.

Cogging torque is non-uniform torque on a rotor caused by the tendency of the rotor to prefer certain discrete angular positions. It is produced by the interaction between the rotor poles and the stator structure and is independent of the load current. Under dynamic condition, the resultant pulsating torque can be transmitted from the rotor to the load, causing undesirable speed pulsations and sometimes, through the stator frame, inducing vibration, possible resonance, and acoustic noise. Because of the sensitivity to speed pulsation of many applications, and the emergence of high energy-product magnets, which aggravate the problem, cogging torque estimation remains a major concern at the initial design stage.

Since a reliable means of estimating the level of the force imbalance and cogging torque as well as their dependence on the motor design parameters is required, there have been a number of efforts to address the problems. Chuang and Lieu [1997] conducted a parametric analysis to determine the effect of motor geometry on the force imbalance in an 8-pole/9-slot motor by the finite-element method. Liu, et al., [1996] employed an analytical approach to show that the force imbalance is large enough to cause some possible problems to hard disk drives supported by fluid film bearings.

There have also been a number of studies on the calculation of cogging torque and its characteristics. Most studies were concerned with the accuracy of finite-element methods. Jufer [1987] and De La Ree and Boules [1989] proposed analytical torque calculation methods. The difficulty in the calculation comes from including the complex geometry of a motor, especially the stator slot effect. Jufer proposed a gap permeance function to consider the stator slot effect. De La Ree assumed the flux density under the slots to be zero to simplify the calculation. Zhu and Howe [1992] made another effort for analytical prediction of the cogging torque calculation. However their method was a numerical calculation based on an analytical calculation of the air gap field. Ackermann, et al., [1992] presented a design method to reduce the cogging torque by adjusting the width of the poles or the width of the slots. They suggested a possible optimization scheme to reduce the cogging torque.

However, in most analytical approaches based on the virtual energy method, the greatest difficulty lies in calculating the direction and magnitude of the flux density in both the magnet and the airgap regions. This difficulty arises from the flux leakage and fringing at the stator slot openings. The influence of circumferential component of the flux density is as important as that of the radial flux density, since its contribution to the rate of change of energy with the rotor position is as large as that of the radial component of the flux density, according to Hwang [1997]. The purpose of this study is to develop an analytical model capable of predicting both the force imbalance and cogging torque and to examine the effect of different physical parameters of the motor on those forces as well. Explicit forms of the force imbalance and cogging torque expressions are derived based on a two dimensional model taking account of the effects of the stator slots and flux fringe, which allows both the radial and the circumferential components of the flux density in the air gap to be included. The Maxwell stress method can be directly used for the force calculation. Dynamic characteristics of the force imbalance and cogging torque are explained in terms of the frequency contents.

II. Force Imbalance and Cogging Torque

A. Maxwell Stress Method

Assuming the effect of magneto-striction is negligible for most motors, the magnetically induced stresses can be represented in terms of the magnetic flux density alone from Woodson and Melcher [1985],

$$\sigma_{ij} = \frac{1}{\mu_0}\left(B_i B_j - \frac{1}{2}\delta_{ij} B_k B_k \right). \tag{1}$$

Magnetic force is produced at the boundaries where magnetic material properties change. Because the permeability of the permanent magnet is approximately that of air, the stresses computed in the air gap largely reflect the stresses on the stator teeth. For a two dimensional analysis in cylindrical coordinates, the magnetic forces acting on the stator surface have the following representations:

$$f_r \approx \sigma_{rr}^{air} = \frac{1}{2\mu_0}\left(B_r^2 - B_\theta^2 \right), \tag{2}$$

$$f_\theta \approx \sigma_{r\theta}^{air} = \frac{1}{\mu_0} B_r B_\theta , \tag{3}$$

where B_r and B_θ are the radial and circumferential flux density components in the air gap. Equations (2) and (3) express the radial and circumferential component of the magnetically induced force stress, respectively. The stresses are then integrated to determine the resultant forces, F_x, F_y and T_z which are the x- and y-component of the force imbalance and the cogging torque, respectively,

$$F_x = l_e \int_C \left\{ \sigma_{rr}^{air} \cos\theta - \sigma_{r\theta}^{air} \sin\theta \right\} d\Gamma , \tag{4}$$

$$F_y = l_e \int_C \left\{ \sigma_{rr}^{air} \sin\theta + \sigma_{r\theta}^{air} \cos\theta \right\} d\Gamma , \tag{5}$$

$$T_z = l_e \int_C R \sigma_{r\theta}^{air} d\Gamma , \tag{6}$$

where C is an arbitrary circle in the air gap with radius, R and l_e is the effective axial length of the motor. Usually R is taken as the radial distance from the center of the stator to the centerline of the air gap in a motor with an external rotor. From the equations above, it can be seen that the evaluation of the forces depends on the correct computation of the flux density distribution in the air gap.

B. Calculation of Force Imbalance and Cogging Torque

The radial and circumferential components of the flux density in the air gap are given for a prototype motor by Kim and Lieu [1998]. Fig. 1 compares the flux densities obtained by the analytical calculation and the finite element method. In a two dimensional analysis in cylindrical coordinates, the Maxwell stresses are integrated along an arbitrary circle in the circumferential direction. It is thus convenient to express the flux density components in the following simplified form:

$$\begin{aligned} B_r = & \sum_{n=1,3,5\cdots}^{\infty} A_n \cos(np\theta - np\omega t) \\ & + \sum_{n=1,3,5\cdots}^{\infty} \sum_{m=0}^{\infty} B_{nm} \cos\{(np+mq)\theta - np\omega t\} \\ & + \sum_{n=1,3,5\cdots}^{\infty} \sum_{m=0}^{\infty} C_{nm} \cos\{(np-mq)\theta - np\omega t\}, \end{aligned} \tag{7}$$

$$\begin{aligned} B_\theta = & \sum_{n=1,3,5\cdots}^{\infty} D_n \sin(np\theta - np\omega t) \\ & + \sum_{n=1,3,5\cdots}^{\infty} \sum_{m=0}^{\infty} E_{nm} \sin\{(np+mq)\theta - np\omega t\} \end{aligned}$$

$$+\sum_{n=1,3,5\cdots}^{\infty}\sum_{m=0}^{\infty}F_{nm}\sin\{(np-mq)\theta-np\omega t\}\,, \tag{8}$$

where A_n, B_{nm}, C_{nm}, D_n, E_{nm}, and F_{nm} are independent of θ and given by Kim and Lieu [1998].

Performing integration (4), (5), and (6) with the aid of orthogonality of the trigonometric functions yields the closed-form expressions of the force imbalance and cogging torque, which are too messy to be presented explicitly in the paper,

$$F_x=\frac{\pi R l_e}{2\mu_0}\sum\left(\sum_n\sum_m\sum_k\sum_l f_{nmkl}^{x}\right)\cos(n\pm k)p\omega t\,;\ \text{for }(n\pm k)p\pm(m\pm l)q=\pm 1\,, \tag{9}$$

$$F_y=\frac{\pi R l_e}{2\mu_0}\sum\left(\sum_n\sum_m\sum_k\sum_l f_{nmkl}^{y}\right)\sin(n\pm k)p\omega t\,;\ \text{for }(n\pm k)p\pm(m\pm l)q=\pm 1\,, \tag{10}$$

$$T_z=\frac{\pi R^2 l_e}{\mu_0}\sum\left(\sum_n\sum_m\sum_k\sum_l f_{nmkl}^{z}\right)\sin(n\pm k)p\omega t\,;\ \text{for }(n\pm k)p\pm(m\pm l)q=0\,, \tag{11}$$

where f_{nmkl}^{x}, f_{nmkl}^{y}, and f_{nmkl}^{z} are the amplitude of the forces that are the combinations of A_n, B_{nm}, C_{nm}, D_n, E_{nm}, and F_{nm} and the indices in the above equations follow $n,k=1,3,5,\cdots$ and $m,l=0,1,2,\cdots$. The explicit equations can obtained from Kim and Lieu [1998]. Note that force imbalance and cogging torque are evaluated only for the frequency components satisfying the right hand side equations, and vanish otherwise by the orthogonality of the trigonometric functions.

III. Comparison of Analytical Predictions and Finite Element Results

A. Force Imbalance

Magnetically non-symmetric DC motors, such as the 8-pole/9-slot design, are often used in applications that call for low cogging torque. The 8-pole/9-slot motor is the common design extensively used in disk drive spindles but has very high force imbalance which would cause ball bearing wear and acoustic noise. Accordingly, it would be harmful to the fluid bearing system supporting the spindle motor. Fig. 2 shows the force imbalance components computed by the analytical and finite-element method for an 8-pole/9-slot motor, with PM slot of 8 degrees, and slot angle of 8 degrees. For a unit motor length, the force imbalance components in x- and y-direction follow those computed by the finite element method in both amplitude and waveform. The maximum error between the two methods is less than 10%. The figure shows the frequency of the force imbalance is 8 times the rotation frequency of the rotor and rotates clockwise, which is the opposite to the rotation of the rotor. This result is consistent with that obtained by Chuang and Lieu [1997]. The computed result indicates that the peak to peak value of this alternating force is about 1.07 N for the effective axial length of 6.3 mm, which is large compared with the total load of the spindle. The variation in amplitude and frequency of the force imbalance could cause stability problems for the case of the spindle motor supported by fluid film bearings, thereby resulting in non-repeatable runout and acoustic problems as well. For this reason, use of the 8-pole/9-slot motor may be limited in the future.

B. Cogging Torque

Fig. 3 shows the cogging torques calculated by the analytical method and the finite element method for a 12-pole/9-slot motor that yields no force imbalance. The figure shows there is a discrepancy in amplitudes between the results. The analytical result underestimates that of the finite element method in amplitude but the frequencies of the cogging torque calculated by both methods agree with each other. The error in cogging torque calculation by the finite element method and analytical method is subject to the accuracy of the field solution, especially the tangential stress component around the corners of the stator teeth. The flux density obtained by the analytical method, which is explained by Kim and Lieu [1998], cannot describe effectively the flux concentration and fringing effect especially at the corners of the stator teeth. This explains a part of the discrepancy. The results would be improved by using a better permeance function that can include the fringing effect.

IV. Dynamic Characteristics of Force Imbalance and Cogging

A. Frequency Contents of Force Imbalance

Force imbalance obtained by the analytical method is given in a harmonic series with the frequency contents in the previous section. The frequency equation which the x- and y-component of the force imbalance must satisfy, can be represented by the following form,

$$(n \pm k)p \pm (m \pm l)q = \pm 1, \tag{12}$$

where $n, k = 1,3,5,\cdots$, and $m, l = 0,1,2,\cdots$.

Note that p is the number of the pole pairs and q is the number of the stator slots, which is usually a multiple number of 3 for typical three phase motors. With the indices given in (12), the frequency equation of the force imbalance reveals several important inferences. Firstly, if the stator slot number is even, no force imbalance is produced in the no-load operation. The deduction of this inference is straightforward from equation (12). The first and second terms of the left-hand side of equation (12) are always even if the stator slot number is even. Then, the frequency equation can be divided by 2, which results in making the right hand side ½. This makes it impossible for the frequency equation to have solutions since the left hand side is still a whole number. Secondly, for this reason, only if the largest common factor (LCF) of the pole and slot number is 1, is force imbalance produced. Thirdly, the frequencies of the force imbalance are always even harmonics of the rotating speed of the rotor since $(n \pm k)p$ are always even. Lastly, the harmonics of the force imbalance are not multiples of one another, nor are they equally separated. For example, Table 1 shows the harmonics of the force imbalance of an 8-pole/9-slot motor. The fundamental harmonic is 8 times that of the rotating speed of the rotor but the higher harmonics are not evenly separated.

Table 1 Frequency contents of the force imbalance of an 8-pole/9-slot motor

Harmonics	Frequency
1 st	$8f_o$
2 nd	$64f_o$
3 rd	$80f_o$
4 th	$136f_o$

f_o = rotating frequency of the rotor

B. Frequency Contents of Cogging Torque

The frequency equation for cogging torque can be represented as follows:

$$(n \pm k)p \pm (m \pm l)q = 0, \qquad (13)$$

where $n, k = 1,3,5,\cdots$ and $m, l = 0,1,2,\cdots$.

The above equation also describes some characteristics of the cogging torque. Equation (13) shows that there always exists cogging torque in all permanent magnet motor since equation (13) always has indices satisfying the frequency equation for arbitrary values of p and q. However, the frequency harmonics depend on the pole and slot number combinations. In fact, the frequencies are harmonics of the least common number of the pole and slot numbers and they are even harmonics of the rotating frequency of the rotor. Table 2 shows the harmonic contents of the cogging torque for external rotor motors used extensively in current disk drive spindle motors. In Table 2, the largest common factor (LCF) indicates how good a spindle motor is in terms of having small cogging torque. The LCF is numerically identical to the number of the slot openings aligning with the pole transitions at a time. Since the maximum cogging torque amplitude occurs at the point where a radial edge of a permanent magnet pole aligns with a radial edge of a stator tooth, the cogging torque is directly proportional to the LCF. However, some motors with different pole and slot number configurations, have, sometimes, the same LCF. For example, the 6-pole/9-slot motor and the 12-pole/9-slot motor have 3 as the LCF whereas their frequency harmonics are different. In this case, the 12-pole/9-slot motor yields less cogging torque than the 6-pole/9-slot motor since, in general, the amplitudes at the harmonics are inversely proportional to the harmonic numbers. The cogging torque shown in Fig. 4 are for the spindle motors with the same dimensions but different pole and slot number combinations with no dead angles. Note that the maximum amplitude of the cogging torques is proportional to the LCF. For the case of motors having the same LCF, Fig. 5(a) shows that motors with higher harmonics have less cogging torque, as explained in the above. Fig. 5(b) shows that the LCF is the stronger indicator for predicting the magnitude of the cogging torque than the harmonic contents. The 8-pole/12-slot motor and the 8-pole/6-slot motor have the same harmonics but Fig. 5(b) shows that the latter has less cogging torque than the former because of the lower LCF. Therefore, the design of a dynamically high performance spindle motor can be obtained by a careful choice of the pole and slot number combinations. The examination of the largest common factor of the pole and slot numbers together with the cogging torque harmonic contents, is a fast and direct criterion for the judgment.

Table 2 Frequency contents of cogging torque of spindle motors

Harmonics	8p/9s	6p/9s	12p/9s	8p/6s	8p/12s
1 st	$72f_o$	$18f_o$	$36f_o$	$24f_o$	$24f_o$
2 nd	$144f_o$	$36f_o$	$72f_o$	$48f_o$	$48f_o$
3 rd	$116f_o$	$54f_o$	$108f_o$	$72f_o$	$72f_o$
4 th	$288f_o$	$72f_o$	$144f_o$	$96f_o$	$96f_o$
LCF	1	3	3	2	4

f_o = rotating frequency of the rotor

V. Conclusion

An analytical method is developed to determine the characteristics of the force imbalance and cogging torque in a permanent magnet motor of surface-mounted magnet types. The method takes advantage of the knowledge of the flux density distribution in the air gap as a function of design parameters. The analytical method provides a fast design and analysis tool for evaluating magnetic forces that are a very time-consuming task if finite-element methods are used.

Force imbalance in the radial direction of the most widely used 8-pole/9-slot spindle motors is one of the main issues concerning ball bearing wear and non-repeatable runout, as well as acoustic and vibration problems. The frequency equation of force imbalance shows that force imbalance is produced only if the largest common factor of the pole and slot number combination is 1. An 8-pole/9-lot motor is an example for this case. The fundamental frequency of the motor is 8 times the rotational frequency of the rotor and it rotates opposite to the rotation of the rotor, which could cause vibration of the rotor system. The fundamental frequency component of the force imbalance magnitude is dominant in the 8-pole/9-slot motor since the other harmonics are located at much higher frequency region on the spectrum. It is also shown that its higher harmonics are not equally separated.

Cogging torque always exists in a permanent magnet motor with slotted stators according to the frequency equation suggested in the study. The frequencies of cogging torque are harmonics of the least common number of the pole and slot numbers, which is always even. The maximum amplitude of cogging torque is related with the number of slot openings aligning with the pole transitions at a time, which is numerically equal to the largest common factor of the pole and slot numbers. Therefore, the largest common factor can be a fast and direct criterion for how good a spindle motor is in terms of having small cogging torque. However, sometimes motors with different pole/slot number combinations can have the same largest common factor. In this case, the harmonic contents of the frequency spectrum should be examined since the amplitude of the cogging torque frequency spectrum is inversely proportional to the order of the harmonics. Therefore, the motor with higher harmonic contents is recommended for lower cogging torque magnitude.

References

Chao, Z. J. Liu, and T. S. Low, "Unbalanced magnetic pull in synchronous machines - Its relation with stator teeth and armature winding," *Proceedings of IMCSD*, 1996, pp. 79-84.

Chuang, T.Y., Lieu, D.K., "Magnetically Induced Vibration in an 8-Pole, 9-Slot Brushless D.C. Motor," *ASME Advances in Information Storage Systems*, 1997.

Liu, Z. J., Bi, C., Zhang, Q. D., Jabbar, M. A., and Low, T. S., "Electromagnetic design for hard disk drive spindle motors with fluid film lubricated bearings," *IEEE Transactions on Magnetics*, Vol. 32, No. 5, Sep. 1996, pp. 3893-3895.

Jufer, M., "Brushless DC motors-gap permeance and PM-MMF distribution analysis," *Proceedings of IMCSD*, 1987, pp. 21-25.

De La Ree, J., and Boules, N., "Torque production in permanent-magnet synchronous motors," *IEEE Transactions on Industry Applications*, Vol. 25, No. 1, 1989, pp. 107-112.

Zhu, Z. Q., and Howe, D., "Analytical prediction of the cogging torque in radial-field permanent magnet brushless motors," *IEEE Transactions on Magnetics*, Vol. 28, No. 2, March 1992, pp. 1371-1374.

Ackermann, B., Janssen, J., Sotteck, R., and Van Steel, R., "New technique for reducing cogging torque in a class of brushless D.C. motors," *IEE Proceedings-B*, Vol. 139, No. 4, 1992, pp. 315-320.

Hwang, S.M., "Effect of co-energy variation on cogging torque in permanent magnet motors," *Proceedings of IMCSD*, 1997, pp. 129-133.

Woodson, H., and Melcher, J., *Electromechanical Dynamics, Part II : Fields, Forces and Motion*, The Robert E. Krieger Publishing Company, New York, 1985.

Kim, U., and Lieu, D. K., “Magnetic field calculation in permanent magnet motors with rotor eccentricity: with slotting effect considered,” *IEEE transactions on Magnetics*, Vol. 34, No. 4, Jul 1998, pp. 2253-2266.

U. Kim, “Analysis of the magnetic field and vibration of permanent magnet motors with rotor eccentricity”, Ph.D. Thesis, University of California at Berkeley, Department of Mechanical Engineering, Dec. 1997.

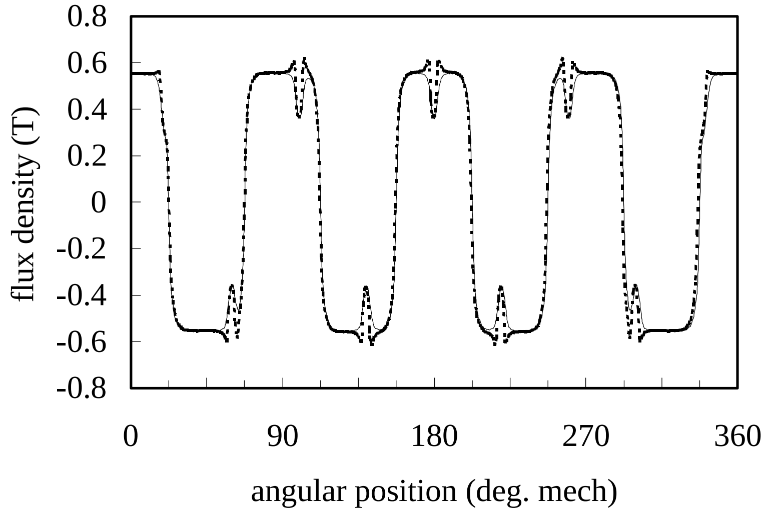

(a)

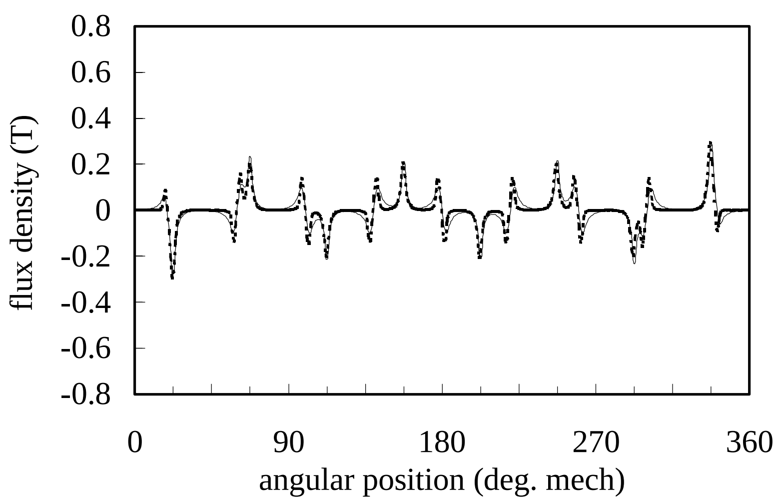

(b)

Fig. 1. Flux density distributions in the middle of the air gap. (a) Radial flux density. (b) Circumferential flux density. Solid lines : analytical results; dotted lines : FEM results.

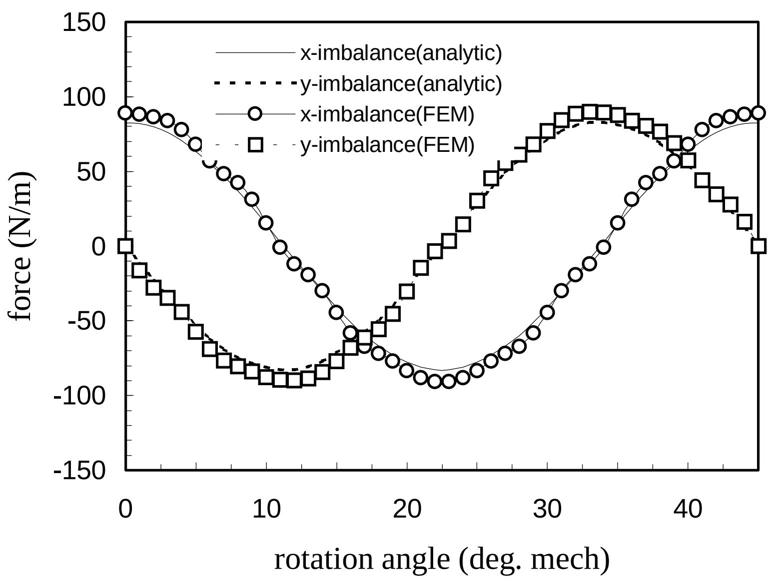

Fig. 2. Force imbalance in an 8-pole/9-slot motor

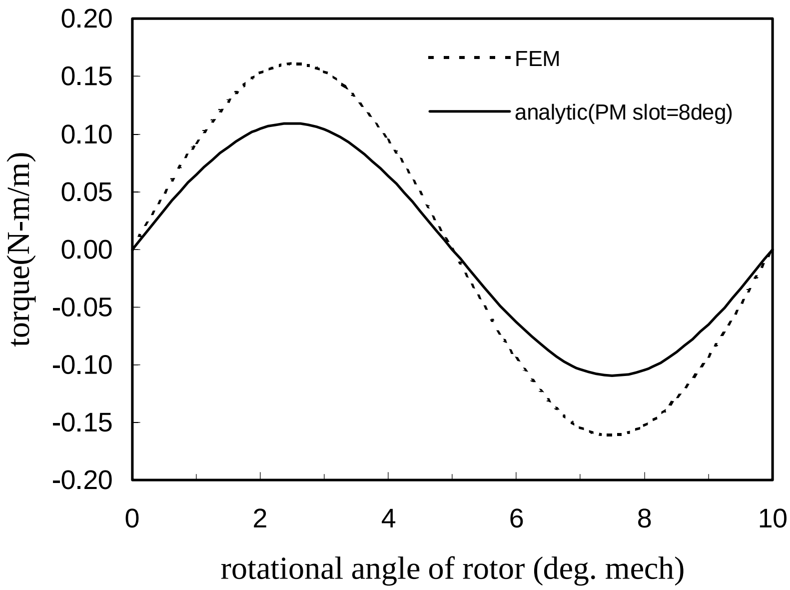

Fig. 3. Cogging torque computed by the finite element method and by the analytical method for a 12-pole/9-slot motor with a tooth slot angle of 8 degrees and the pole slot angle of 8 degrees.

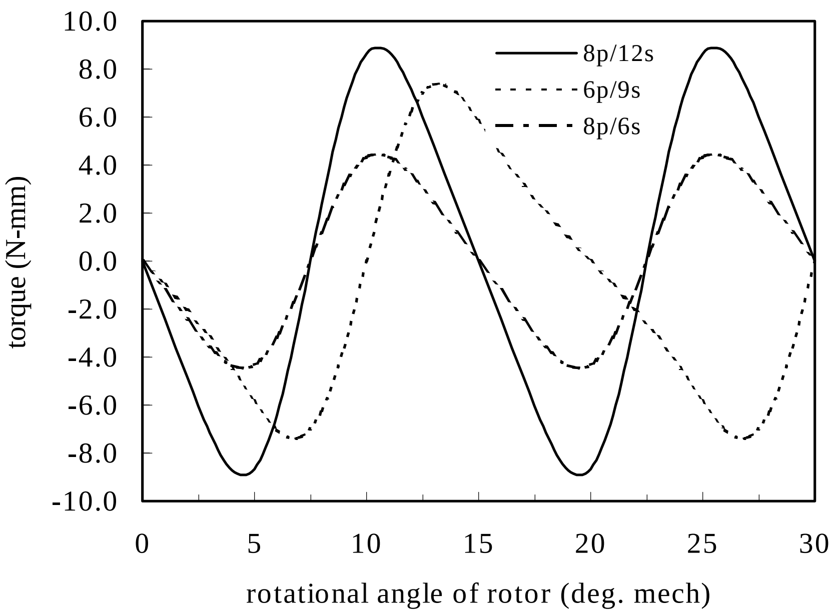

Fig. 4. Cogging torque of spindle motors with different pole/slot combinations.

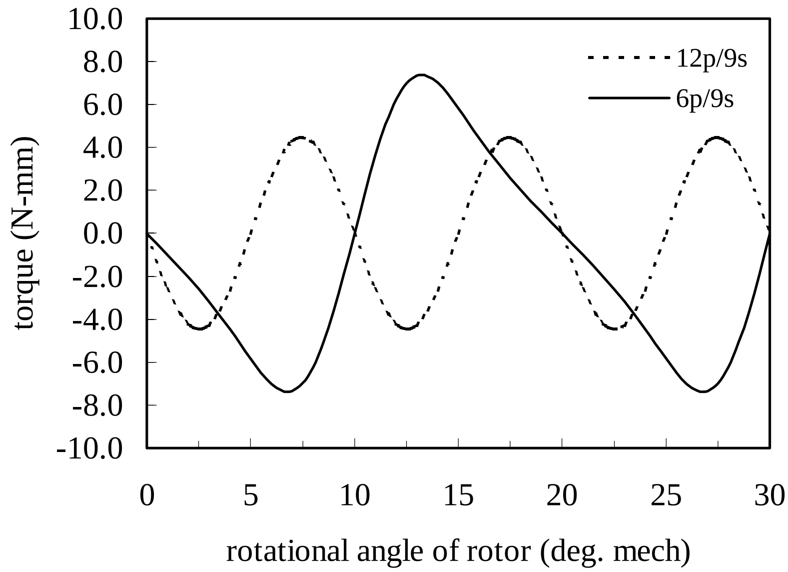

(a)

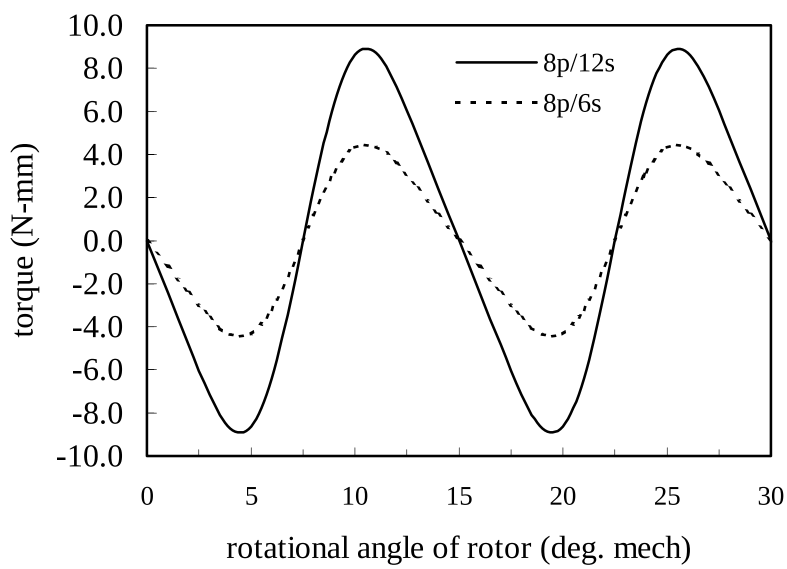

(b)

Fig. 5. Cogging torque comparison of different pole/slot number combinations
(a) for the case of the same LCF but different harmonics.
(b) for the case of the same harmonics but different LCF.